[CANCER RESEARCH 33, 1608–1614, July 1973]

The Ultrastructure of Renal Neoplasms Induced by Aflatoxin B_1[1]

Leonard P. Merkow, Sheldon M. Epstein,[2] Malcolm Slifkin, and Matias Pardo

The Division of Experimental Pathology, William H. Singer Memorial Research Institute of the Allegheny General Hospital, Pittsburgh, Pennsylvania 15212 [L. M., M. S., M. P.], and Department of Pathology, School of Medicine, University of Pittsburgh, Pittsburgh, Pennsylvania 15213 [S. M. E.]

SUMMARY

A significant incidence of renal carcinomas was noted in male Wistar rats fed diets containing 1.0, 2.0, or 3.0 ppm of purified aflatoxin B_1. An ultrastructural study of these kidney epithelial neoplasms was performed. Although the component tumor cells preserved some characteristics consistent with a renal origin, additional features usually characteristic of malignant cells were noted. Among the latter, the most striking were loss of apical orientation of brush borders and a lack of orientation of mitochondria. The observations are compatible with a tubular origin for these malignant neoplasms and may serve to make this tumor of use as a tool for the study of specific macromolecular and/or organelle alterations during and subsequent to the oncogenic process.

INTRODUCTION

An unanticipated high incidence of renal epithelial neoplasms was encountered in earlier experiments when male Wistar rats ingested low levels of the potent carcinogen aflatoxin B_1 (5). Because this kidney tumor resembled human renal cell adenocarcinoma, and since renal tumors had been noted by others (*cf.* Ref. 5) following experimental aflatoxin regimens, and also because of widespread human exposure to oncogenic mycotoxins (Refs. 1 and 2; *cf.* Ref. 5), further study of these experimental renal tumors was more systematically pursued. Additionally, it appeared in our initial study (5) as if the cells within the tumor were often homogeneous and formed "brush borders" (5). If this were so, then this tumor could potentially be a valuable source for *such* material. For these reasons, an ultrastructural study of this lesion was performed and the accrued observations are the subject of this communication.

[1] Supported in part by grants from the American Cancer Society, Inc., and the Beaver County Cancer Society; and by USPHS Research Grants CA 06074 and CA 10667 from the National Cancer Institute, AM 05644 from the National Institute of Arthritis and Metabolic Diseases, and GM 135 (a training grant) and GM 10269 (a research grant) from the National Institute of General Medical Sciences and Contract PH-4363 505.

[2] Recipient of a Career Development Research Award (K-3-CA-15-245) from the National Cancer Institute. Present address: Department of Pathology, Indiana University School of Medicine, Indianapolis, Ind. 46202.

Received April 3, 1972; accepted March 16, 1973.

MATERIALS AND METHODS

Animals and Diets. Wistar strain male rats (Carworth Farms, New City, N. Y.), weighing 150 to 200 g were used and maintained as described (5). Highly purified aflatoxin B_1 generously supplied by Dr. G. N. Wogan (Department of Nutrition and Food Science, Massachusetts Institute of Technology) was added to the basal control diet as detailed previously (5). The aflatoxin-containing diets were prepared and fed for the same time as in the initial study (5). However, in the current experiments, levels of 1.0, 2.0, and 3.0 ppm of the mycotoxin were used.

Experimental Design. This varied somewhat from that used previously (5) since it was necessary to sacrifice the animals at a selected interval in order to obtain fresh viable tissue for study. Therefore, in these experiments, rats were killed 391 days after initiation of the dietary regimens. Twelve rats were fed each level of aflatoxin B_1 and 9 animals were provided with a basal control diet only for use in the current experiments.

For Light Microscopy. Portions of tissue from the renal neoplasms were fixed in neutral buffered formaldehyde solution. After fixation, tissues were dehydrated, embedded in paraffin blocks, and sectioned at 5 to 6 μm. Sections were stained with hematoxylin and eosin.

For Electron Microscopy. For the ultrastructural study, renal tumor tissue was obtained from 3 rats given 3.0 ppm aflatoxin B_1 diet and fasted for 24 hr prior to sacrifice. Additionally, tissue was obtained from 2 animals that had ingested 2.0 ppm of aflatoxin B_1 and from 1 animal on the 1.0-ppm aflatoxin regimen. Thus, detailed electron microscopic observations of tumor tissue obtained from 6 separate animals were performed. Sixteen to 20 Epon-embedded blocks of tissue were prepared from each tumor (1-μm methylene blue-stained sections were examined from every block). Grids for detailed ultrastructural examination (thin sections) were prepared from only 6 to 10 blocks for each of the 6 different cancers. However, since the appearance of these lesions did not differ from those tumors occurring in the kidneys of rats on the highest dosage of aflatoxin, for ease of presentation, only data from the 3.0-ppm groups are detailed. Autopsy was performed 391 days after initiation of the experiment. A similar number of control rats were used and their tissue was handled similarly to tissues obtained from the experimental group. However, grids for ultrastructural examination were prepared from only 3 to 4 blocks for each one of the control animals.

Samples of tissue from the kidney neoplasms and normal kidneys were placed in cold (4°) 3% glutaraldehyde and 0.1 M phosphate buffer (pH 7.4) containing 1% calcium chloride. After 4 hr, the tissues were washed in 0.1 M phosphate buffer (pH 7.4), cut into 1-mm cubes, and postfixed in 1% osmium tetroxide in 0.1 M phosphate buffer (pH 7.4) with sucrose. The resultant cubes of tissue were kept refrigerated in the above fixture for 1 to 2 hr. Dehydration was performed through a graded sequence of ethanols (15 min each in 50, 70, 95, 100, 100, and 100%). The samples were then placed in propylene oxide for 2, 15-minute changes. Infiltration of tissue was carried out with 1 change of 50% propylene oxide: 50% epoxy resin for 1 hr followed by pure epoxy resin overnight. The tissue was then embedded in epoxy resin (Epon 8.2). Sections 1 μm thick were prepared and stained with methylene blue for light microscopy. Sections displaying silver or gold interference colors were obtained with an ultramicrotome (Porter-Blum MT-1 or MT-2) equipped with glass knives. Ultrathin sections were stained with a 5% solution of uranyl acetate followed by lead citrate. Thin sections were examined with a Philips EM-300 electron microscope at 60 kV.

RESULTS

Renal neoplasms similar in gross and light microscopic appearance to those described previously (5) were present in 50% (6 of 12) of the animals fed 3 ppm of aflatoxin B_1. The incidence of grossly and microscopically evident renal tumors was 25% (3 of 12 in each group) in animals fed either 1.0 or 2.0 ppm regimens (5). Neither the gross appearance of these lesions nor their histopathology when paraffin block sections were studied differed from that noted earlier (5). The tumors were quite homogeneous from animal to animal and, as previously described, acinar formations and papillary fronds were often noted (5). Frequently, the luminal margins of the malignant epithelial cells were somewhat serrated causing a "brush border"-like appearance (Figs. 3 and 4; Ref. 5).

The histology and ultrastructure of control animal kidneys did not present any unusual characteristics and so details of the control observations are not elaborated.

Epon-embedded 1-μm-thick sections of renal tumor tissue showed well-differentiated epithelial cells most frequently arranged as papillary fronds supported by a thin core of connective tissue (Fig. 1). Often small vessels within the tumors were invaded by neoplastic epithelial cells (Fig. 1, *Inset a*). Individual tumor cells tended to be either light or dark with the former often being more prominent at the distal tip (edge) of a papillary frond (Fig. 1). These nuclei and their nucleoli were usually uniform in size, shape, and staining affinity (Fig. 1, *Inset b*). However, despite the general uniformity, in rare areas, mitotic figures and occasional cells with 1 or more large dense nucleoli (Fig. 1) and some widely scattered hyperchromatic variable-sized nuclei were seen. The ultrastructural study (which, in the main, is detailed below) of the nucleoli revealed no significant reproducible abnormalities, and normal qualitative and quantitative interrelationships of this organelle were preserved. Some nuclei were observed to have irregular shapes and occasional nuclei with foci of sharp angulations rather than a more uniformly curved contour were seen. Infrequently, nuclear chromatin appeared excessively aggregated by the nuclear envelope but this feature was not prominent. Rarely apparent reduplications of small portions of the nuclear envelope were seen but most often the nuclear membranes were unremarkable. Tumor cells had an abundant cytoplasm either finely and homogeneously granular or containing multiple small cytoplasmic vacuoles (Fig. 1, *Inset b*). In tumor areas with an acinar or tubular pattern, both the histological and cytological appearance of the cells was similar to that previously reported (Figs. 1 to 5; *cf.* Ref. 5).

It became evident from the study of survey electron micrographs that the tumor cells retained a considerable degree of differentiation. Nonetheless, inter- and intracellular relationships were reproducibly altered in a variety of respects (Figs. 2 to 4). Although numerous microvilli were evident, these appeared at all surfaces of the epithelial cells with no predilection for an apical orientation (Fig. 3). Such villous projections, when present at the luminal margin of cells, undoubtedly contributed to such cells appearing to have "brush borders" when they were studied with light microscopy. These finger-like cellular projections merged with other types of specialized attachment sites of the plasmalemma (Figs. 2 to 5). Infolding of the plasmalemma was also noted (Fig. 6). However, such infoldings neither encircled mitochondria nor tended to be in proximity to basement membrane-like material. Furthermore, subapical vacuoles and tubular invaginations were not usually associated with microvilli (Figs. 2 to 4). Some areas of the tumor contained abundant material simulating thickened basement membrane-like material (Fig. 4). This material consisted of amorphous dense deposits, in irregular array, devoid of recognizable orientation at the basal portion of the neoplastic cells. Higher magnification of these amorphous dense extracellular areas disclosed no reproducible substructure although their electron opacity would tend to preclude optimal resolution in the sections available for study. Nonetheless, the basic amorphous nature of the extracellular dense material is not inconsistent with its being similar to renal tubular basement membrane. Occasionally, a variety of cellular organelles in variable degrees of preservation was seen in an extracellular locus most often closely associated with the dense material described above. Mitochondria were generally distributed throughout the tumor cell cytoplasm and not concentrated in any specific locus (Figs. 2 to 8). In many mitochondria, the granular matrix was largely absent and this resulted in a vesicular appearance (Figs. 2 to 6). Nonetheless, lamelliform cristae were observed (Figs. 2 to 9). Well-defined myelin figures were frequently noted within mitochondria (Figs. 6 and 7). Such figures quite possibly are due to fixation (4). Such dense laminated structures were often circumscribed by a well-defined membrane (Fig. 6, *inset*). Many ribosomes were scattered throughout the cytoplasm and these often formed polysomes. Rough endoplasmic reticulum in parallel or nonparallel array was a common cytoplasmic organelle (Figs. 3 and 5 to 7). Numerous densely osmiophilic, irregularly shaped, diminutive electron-opaque cytoplasmic structures often lacking both a discernible substructure and definite diagnostic features were consistent with the appearance of lysosomes (Figs. 3 to 5). Occasional clusters of monoparticulate glycogen were observed (Fig. 6). Vacuoles containing lipid were not a major finding. Microbodies were also observed in the tumor

cells (Fig. 7). Well-developed Golgi complexes (Figs. 4, 7 and 8) and multivesicular bodies (Fig. 6, *inset*) were seen. No definitive evidence was obtained that the extracellular amorphous dense material represented Golgi secretions.

All cells studied had a large variety of well-distributed organelles.

DISCUSSION

The current ultrastructural observations confirm the light microscopic suggestion (5) that cells within this renal tumor induced by aflatoxin B_1 contain abundant brush borders. The incidence of kidney neoplasms in our experiments appears dependent upon the cumulative dose of aflatoxin. Data of other investigators (7) strongly suggest a similar dose-response relationship between the total intake of aflatoxin and the incidence of renal epithelial tumors. The current findings also support our prior report (5) that the kidneys of Wistar rats are especially prone to develop renal neoplasia when exposed to aflatoxin B_1. Wogan *et al.* (8) have confirmed the earlier work of others (*cf.* Ref. 3) that aflatoxin G_1 has a more marked renal oncogenic effect in some strains of rats than does aflatoxin B_1. However, our results appear to demonstrate a specific effect of aflatoxin B_1 that is *not* due to contamination with another mycotoxin. This is true, since the aflatoxin B_1 that we used was of high purity. Moreover, in unpublished experiments we *failed* to find any renal tumors in Fischer rats, a strain susceptible to the development of renal adenocarcinoma when given aflatoxin G_1 (8), when concurrently exposed with the Wistar rats to aflatoxin B_1.

Our past and current studies offer no firm evidence relating to the histogenetic sequence of events occurring during the process of renal oncogenesis associated with aflatoxins. However, others (3) have reported that "large bizarre" cells are noted in the straight segments of the proximal tubules of male Porton rats 3 to 4 weeks after the animals received acute toxic doses of aflatoxin G_1. The overt malignant nature of the cells investigated in the current study precludes dogmatic statements as to their site of origin within the renal tubule. However, we did observe microvilli, possible basement membrane-like material, a variety of types of cell junctions, a well-developed Golgi complex, smooth endoplasmic reticulum, rough endoplasmic reticulum, cytosomes, and occasional multivesicular bodies in the malignant renal epithelial cells. These cytological features do not preclude the possibility that the tumors arose either *in toto* or partially from the proximal convoluted tubule. The presence of abundant amorphous extracellular basement membrane-like material is also compatible with, although not diagnostic of, a tubular origin for the presently described cancer. In unpublished studies, attempts were made with histochemical procedures to define better the nature of the intercellular dense material. Whereas results such as periodic acid-Schiff-positive staining are consistent with some such material being similar to basement membrane, nonetheless, the lack of irrefutable diagnostic specificity of the applied stains precludes dogmatic assertions.

Specific mention should be made of the lack of orientation of the brush borders seen in the malignant renal epithelial cells. Others have mentioned that, in benign renal adenomas, brush borders are noted only at the free surface of cells. Conversely, in both experimental and human renal adenocarcinomas, the brush borders can occur at unusual sites (*cf.* Ref. 6). Our renal neoplasms formed a microvillous surface on any side as well as the luminal border. Thus, it appears that the tumor cells were relatively well differentiated and possessed an increased surface area probably greater than that of normal renal tubular cells. Nevertheless, reabsorption by neoplastic cells may not have been enhanced or, indeed, of a physiological order since the individual tumor cells did not display a normal membrane-mitochondria relationship and were not always associated with a lumen.

REFERENCES

1. Alpert, M. E., and Davidson, C. S. Mycotoxins: A Possible Cause of Primary Carcinoma of the Liver. Am. J. Med., *117:* 325–329, 1969.
2. Bourgeois, C. H., Shank, R. C., Grossman, R. A., Johnsen, D. O., Wooding, W. L., and Chandavimol, P. Acute Aflatoxin B_1 Toxicity in the Macaque and Its Similarities to Reye's Syndrome. Lab. Invest., *24:* 206–216, 1971.
3. Butler, W. H., and Lijinsky, W. Acute Toxicity of Aflatoxin G_1 to the Rat. J. Pathol., *102:* 209–212, 1970.
4. Curgy, J. J. Influence du Mode de Fixation sur la Possibilité d'Observer des Structures Myéliniques dans les Hépatocytes d'Embryons de Poulet. J. Microscop. *7:* 63–80, 1968.
5. Epstein, S. M., Bartus, B., and Farber, E. Renal Epithelial Neoplasms Induced in Male Wistar Rats by Oral Aflatoxin B_1. Cancer Res., *29:* 1045–1050, 1969.
6. Hard, G. C., and Butler, W. H. Ultrastructural Aspects of Renal Adenocarcinoma Induced in the Rat by Dimethylnitrosamine. Cancer Res., *31:* 366–372, 1971.
7. Lee, D. J., Wales, J. H., and Sinnhuber, R. O. Hepatoma and Renal Tubule Adenoma in Rats Fed Aflatoxin and Cyclopropenoid Fatty Acids. J. Natl. Cancer Inst., *43:* 1037–1044, 1969.
8. Wogan, G. N., Edwards, G. S., and Newberne, P. Structure-Activity Relationships in Toxicity and Carcinogenicity of Aflatoxins and Analogs. Cancer Res., *31:* 1936–1942, 1971.

Fig. 1. An aflatoxin-induced renal neoplasm shows typical papillary fronds. Both light- (*arrow*) and dark-staining cells are arranged about small capillaries. Epon-embedded, methylene blue-stained tissue, × 400. *Inset a*, an arteriole adjacent to the neoplasm displays infiltration by tumor cells (*arrows*). × 150. *Inset b*, in focal areas, the neoplastic cells showed a multitude of small intracytoplasmic vacuoles. Such vacuoles may be related to focal aggregates of glycogen (see Fig. 6) although this is somewhat speculative. × 560.

Fig. 2. Adjacent to the lumen (*L*) are several neoplastic cells containing mitochondria (*M*), interdigitating microvilli (*Mv*), and specialized attachment sites (*arrows*). The mitochondria show considerable loss of matrices. The nucleus (*N*), rough endoplasmic reticulum (*Rer*), and lysosomes (*Ly*) are evident. This and all subsequent figures represent glutaraldehyde, osmium-postfixed, Epon-embedded tissue stained with uranyl acetate and lead citrate. × 12,500.

Fig. 3. Several neoplastic cells display numerous interdigitating microvilli (*Mv*) between most apposed surfaces with no predilection for apical orientation. This specialization of the plasma membrane represents the brush borders seen by light microscopy. The microvillous projections are contiguous with other attachment sites, such as tight junctions (*arrows*). A prominent Golgi complex (*Go*), numerous mitochondria (*M*), myelin figures (*Mf*), lysosomes (*Ly*), and numerous microbodies (*Mb*) are evident within a cytoplasm containing free ribosomes (*Rnp*) and short cisternae of nonparalleled rough endoplasmic reticulum (*Rer*). × 10,500.

Fig. 4. A low-power survey view of several neoplastic cells displaying aggregates of dense osmiophilic intercellular material (*Dm*). The neoplastic cells display nuclei (*N*), mitochondria (*M*), Golgi complexes (*Go*), numerous lysosomes (*Ly*) and cisternae of endoplasmic reticulum (*arrows*). Microvilli (*Mv*) are located at a variety of sites. × 6,400.

Fig. 5. Numerous interdigitating microvilli (*Mv*) are contiguous with several tight junctions. The cytoplasm contains an abundance of rough endoplasmic reticulum (*Rer*), mitochondria (*M*), and lysosomes (*Ly*). × 18,000.

Fig. 6. A cluster of monoparticulate glycogen (*Gly*) is adjacent to numerous cisternae of rough endoplasmic reticulum (*Rer*) as well as altered mitochondria (*M*). A large mitochondrion displays invagination of the internal limiting membrane on the *left* and formation of a myelin figure partially replacing the matrix and cristae at the *lower right*. Such myelin figures may be due to fixation (4). Infolding of the plasmalemma (*Pl*) is evident. × 31,500. *Inset*, a mitochondrion associated with a dense membrane-limited body. × 36,000.

Fig. 7. Two mitochondria (*M*) contain myelin figures (as noted above may be due to fixation artifact) replacing the cristae and matrix in focal regions. Numerous lysosomes (*Ly*), a microbody (*Mb*), Golgi complexes (*Go*), rough endoplasmic reticulum (*Rer*), and a nucleus (*N*) are evident. × 24,500.

Fig. 8. A neoplastic cell displays a multitude of Golgi complexes (*Go*). Associated with these organelles are numerous lysosomes (*Ly*). × 20,500.

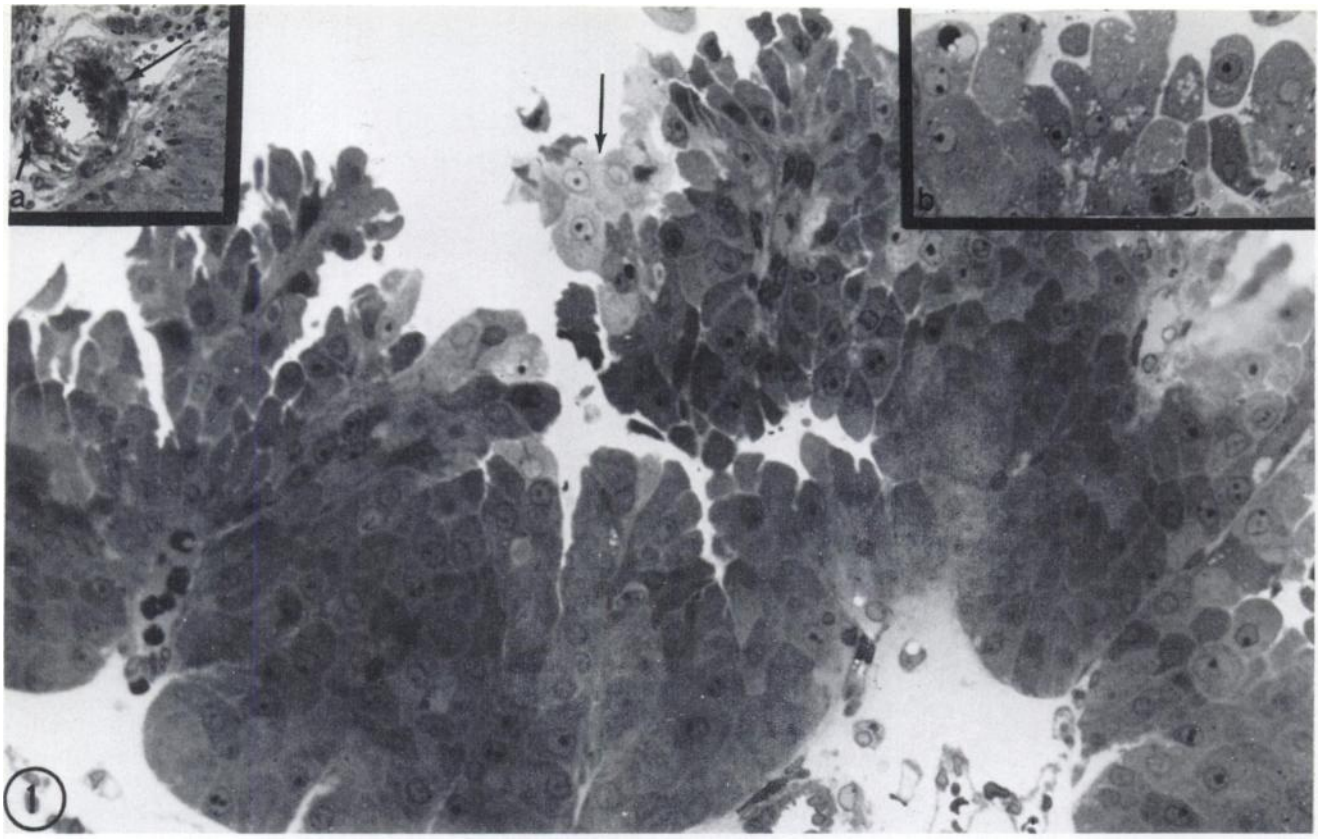
a
b
1

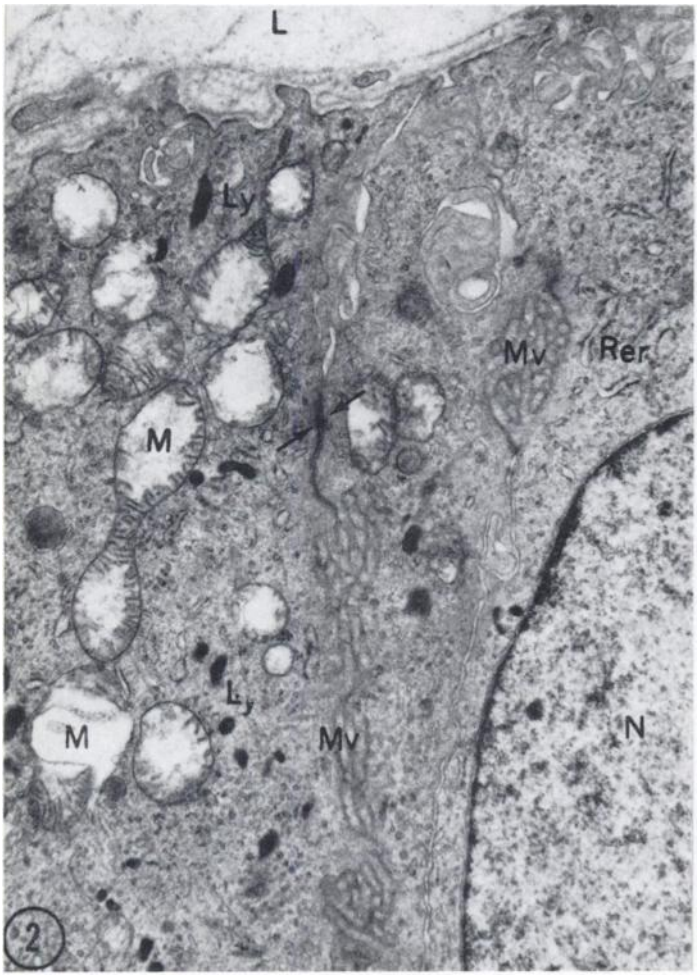
L
Ly
Mv
Rer
M
Ly
M
Mv
N
2

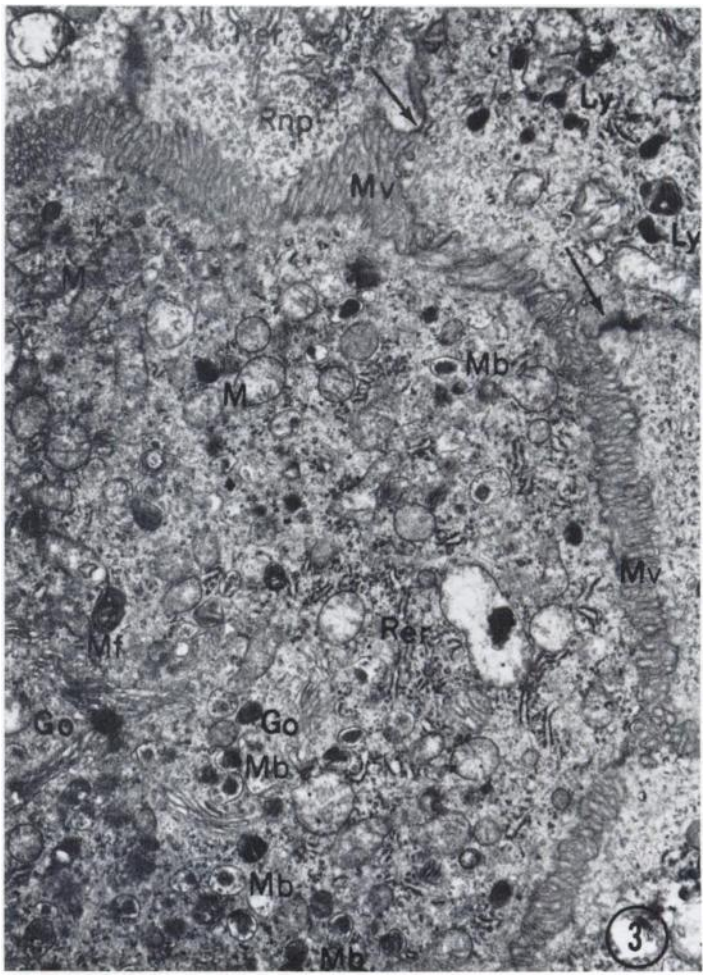
Rnp
Mv
Ly
Ly
M
Mb
M
Mv
Mf
Rer
Go
Go
Mb
Mb
Mb
3

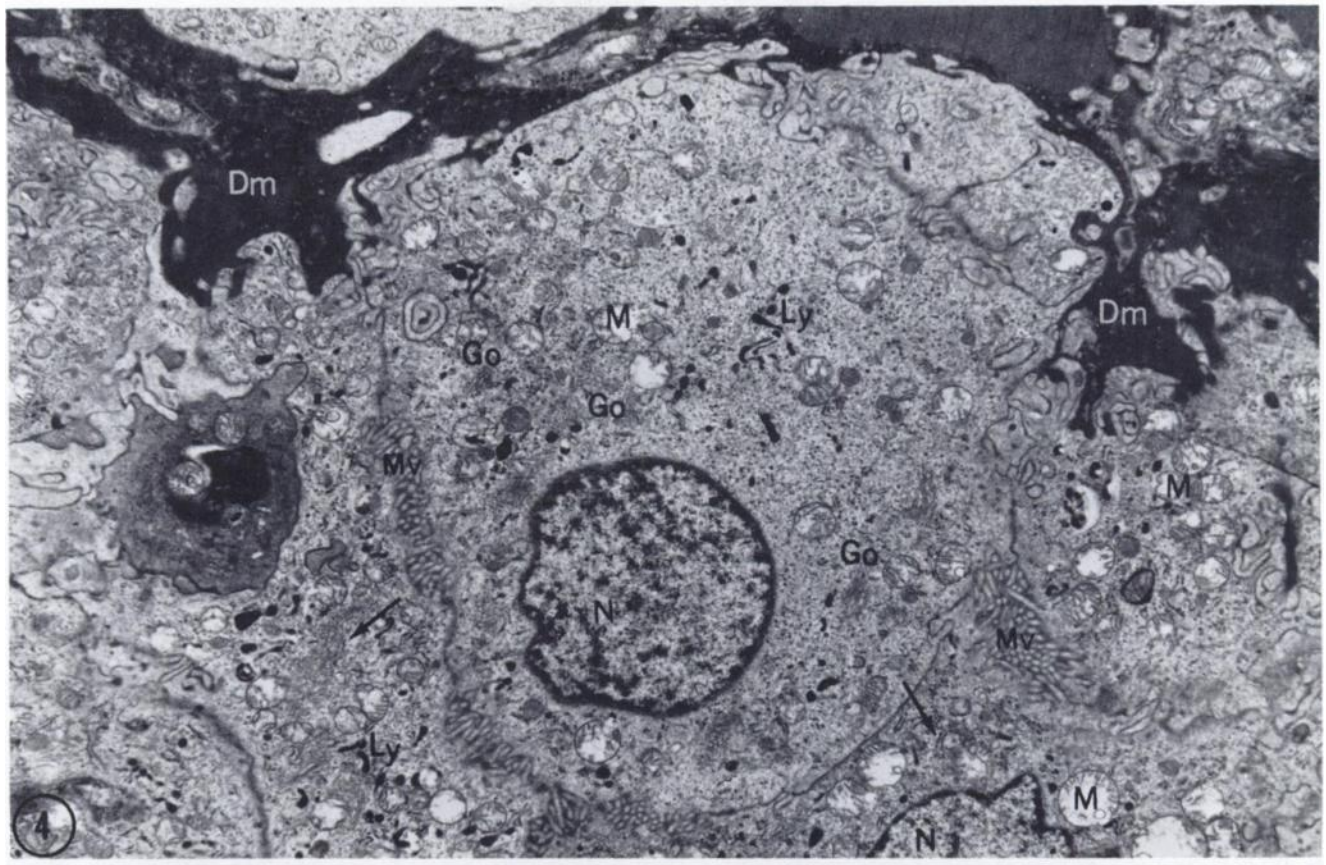
Dm
Dm
M
Ly
Go
Go
Mv
M
Go
N
Mv
Ly
M
N
4

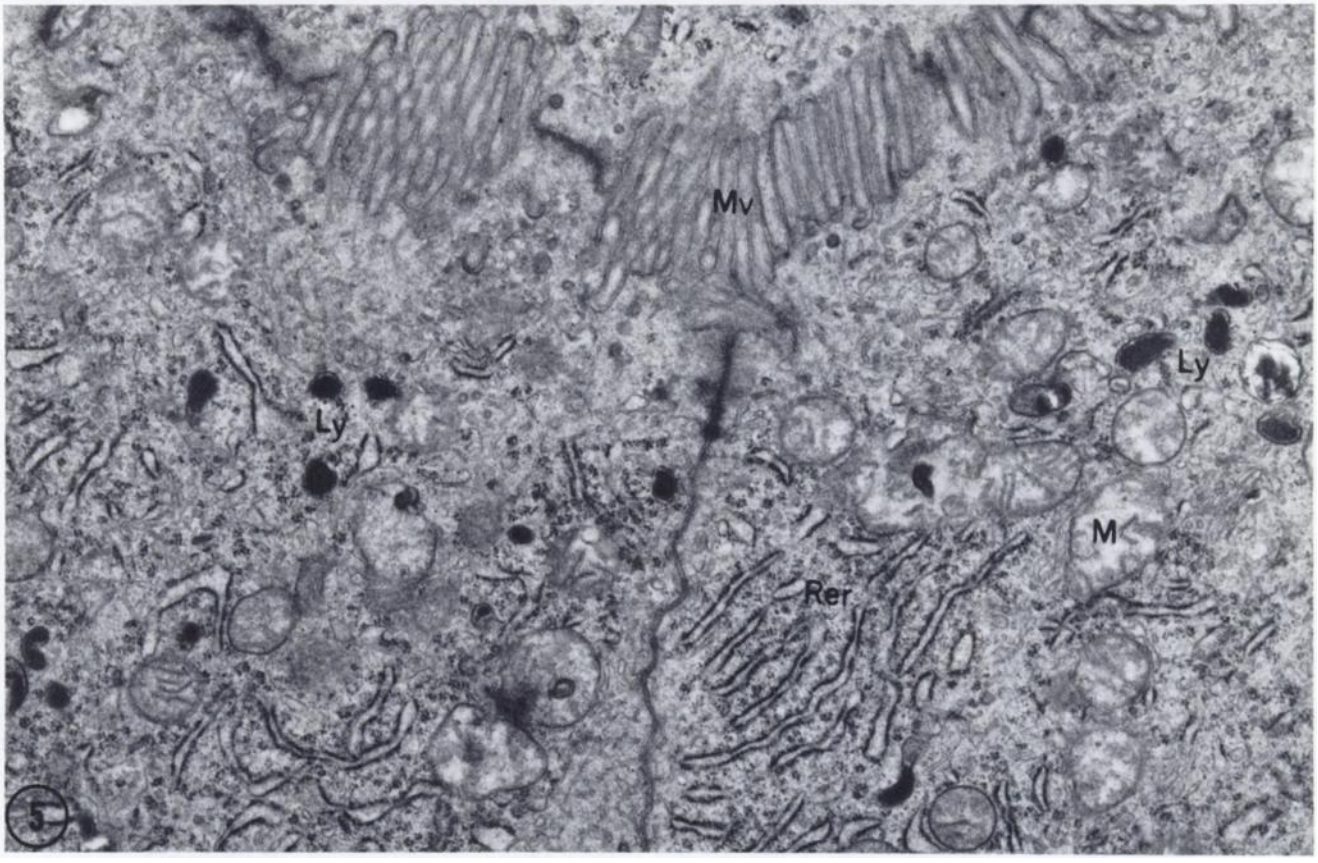
Mv
Ly
Ly
M
Rer
5

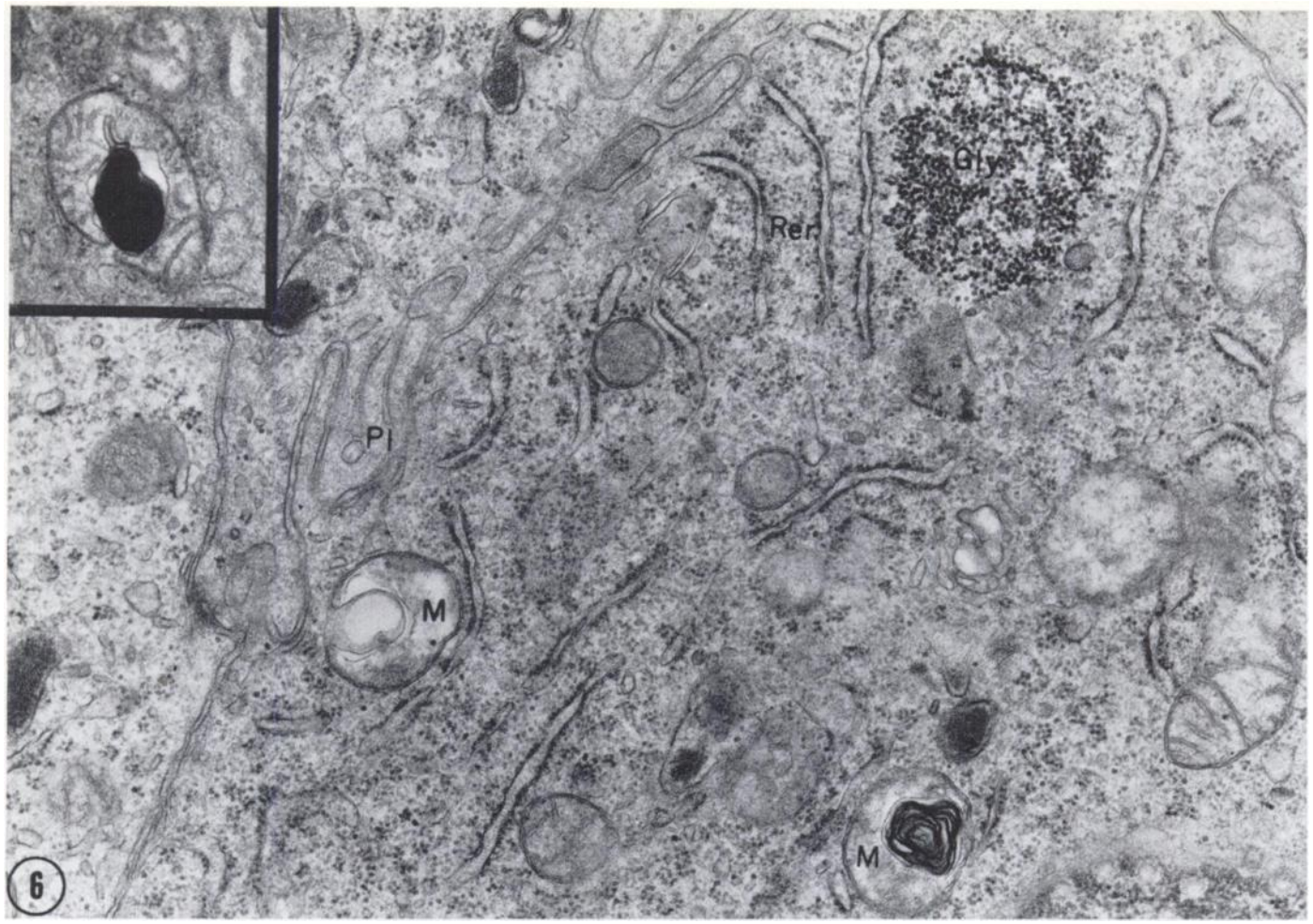
Gly
Rer
Pl
M
M
6

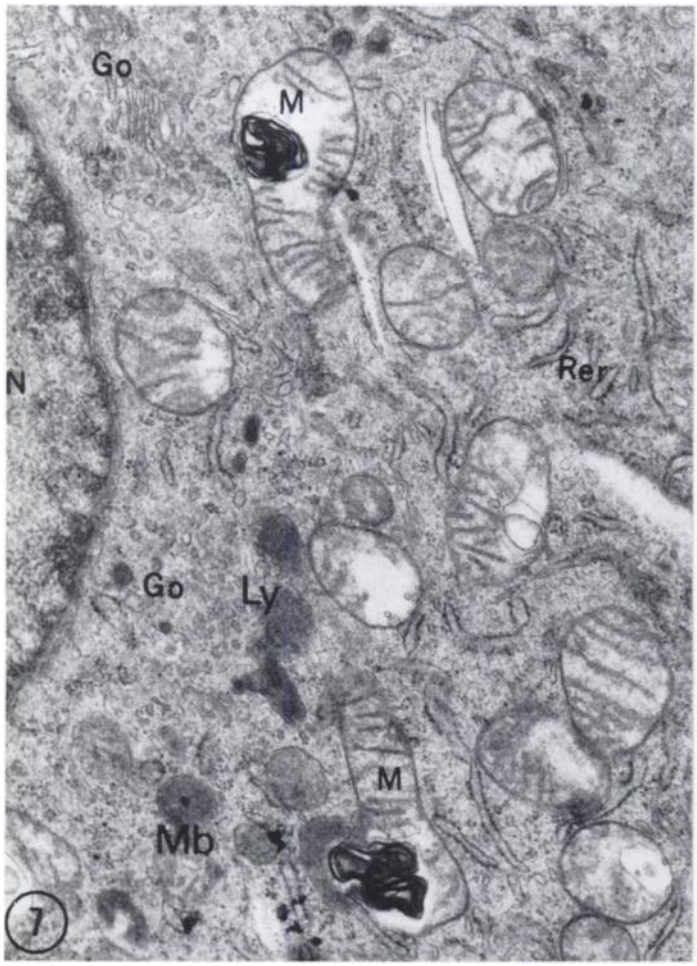
Go
M
N
Rer
Go
Ly
M
Mb
7

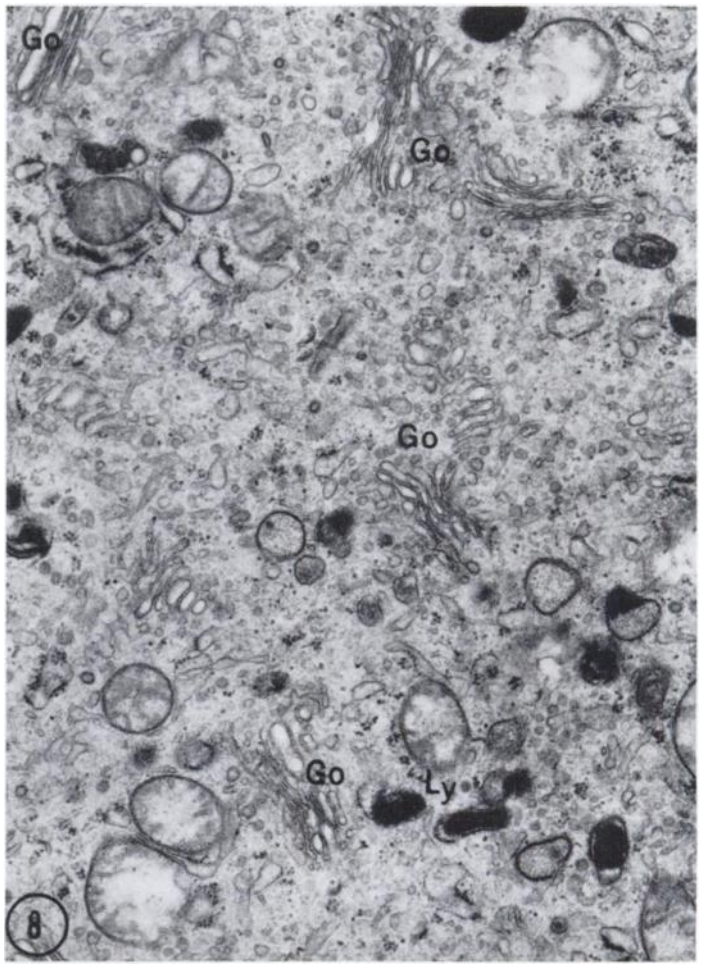
Go
Go
Go
Go
Ly
8